Available online at www.sciencedirect.com
SCIENCE DIRECT®
Biochimica et Biophysica Acta 1610 (2003) 109–123
BIOCHIMICA ET BIOPHYSICA ACTA
BBA
www.bba-direct.com

Downstream coding region determinants of bacterio-opsin, muscarinic acetylcholine receptor and adrenergic receptor expression in *Halobacterium salinarum*☆

Cynthia L. Bartus[a], Veli-Pekka Jaakola[b], Regina Reusch[a], Helene H. Valentine[c], Pirkko Heikinheimo[d], Agata Levay[a], Lincoln T. Potter[c], Heikki Heimo[b], Adrian Goldman[b], George J. Turner[a,*]

[a] *Department of Physiology and Biophysics, and the Neuroscience Program, University of Miami School of Medicine, PO Box 016430, 1600 N.W. 10th Avenue, Miami, FL 33101, USA*
[b] *Structural Biology and Biophysics, Institute of Biotechnology, PO Box 65, University of Helsinki, FIN-00014, Helsinki, Finland*
[c] *Department of Molecular and Cellular Pharmacology, University of Miami School of Medicine, Miami, FL 33101, USA*
[d] *Department of Biochemistry and Food Chemistry, University of Turku, Vatselankatu 2, FIN-20014, Turku, Finland*

Received 29 August 2002; received in revised form 24 October 2002; accepted 4 November 2002

Abstract

The aim of this work is to develop a prokaryotic system capable of expressing membrane-bound receptors in quantities suitable for biochemical and biophysical studies. Our strategy exploits the endogenous high-level expression of the membrane protein bacteriorhodopsin (BR) in the Archaeon *Halobacterium salinarum*. We attempted to express the human muscarinic acetylcholine (M_1) and adrenergic (a2b) receptors by fusing the coding region of the *m1* and *a2b* genes to nucleotide sequences known to direct *bacterio-opsin* (*bop*) gene transcription. The fusions included downstream modifications to produce non-native carboxyl-terminal amino acids useful for protein identification and purification. *bop* mRNA and BR accumulation were found to be tightly coupled and the carboxyl-terminal coding region modifications perturbed both. *m1* and *a2b* mRNA levels were low, and accumulation was sensitive to both the extent of the *bop* gene fusion and the specific carboxyl-terminal coding sequence modifications included. Functional *a2b* adrenergic receptor expression was observed to be dependent on the downstream coding region. This work demonstrates that a critical determinant of expression resides in the downstream coding region of the wild-type *bop* gene and manipulation of the downstream coding region of heterologous genes may affect their potential for expression in *H. salinarum*.

Keywords: G protein-coupled receptor expression; Archaea; Gene fusion

Abbreviations: bop, *bacterio-opsin* gene; Bop, bacterio-opsin protein; BR, bacteriorhodopsin; PM, purple membrane harvested from sucrose gradients containing purified BR; SRI, Sensory Rhodopsin I; bp, base pairs; PCR, polymerase chain reaction; SDS-PAGE, sodium dodecyl sulfate–polyacrylamide gel electrophoresis; A_λ, absorbance at wavelength λ; GPCRs, G protein-coupled receptors; G proteins, guanine regulatory proteins; mAChR, human muscarinic acetylcholine receptor; M_1, M_1 subtype of the human muscarinic acetylcholine receptor; *m1*, gene coding for the M_1 receptor; *m1-bop*, *m1-bop* gene fusions; M_1-Bop, M_1-Bop fusion proteins; a2bAR, human α_2-adrenergic receptor, subtype B; *a2b*, gene coding for the α_{2B}-AR receptor; *a2b-bop*, gene fusions; a2b-Bop, a2b-Bop fusion proteins; 6His, six consecutive histidine amino acids; HA, nine amino acid peptide epitope from the influenza hemaglutinin protein

☆ Support is acknowledged from the American Heart Association Grant-in-Aid (AHA664871), the National Science Foundation (MCB-9817140), the National Institutes of Health (DK60847), a Johnson & Johnson Focused Giving Program Grant (all to G.J.T.), from the Finnish National Technology Agency (Grants 40128/88 and 40272/81, to A.G.) and from the Ella and Georg Ehrnrooth foundation (to V.-P.J.).

* Corresponding author. Tel.: +1-305-243-3189; fax: +1-305-243-5931.
E-mail address: gturner@miami.edu. (G.J. Turner).

0005-2736/03/$ - see front matter © 2003 Elsevier Science B.V. All rights reserved.
doi:10.1016/S0005-2736(02)00710-1

1. Introduction

G protein-coupled receptors (GPCRs) make up the largest gene family identified in eukaryotes [1]. Upon their activation by endogenous ligands or drugs, these receptors interact with G proteins to produce a signal transduction cascade [2], which mediates cellular responses [3]. GPCRs have superficial structural homology with bacteriorhodopsin (BR) in that they have a core of seven transmembrane antiparallel α-helices [4].

Current understanding of GPCR function is limited by knowledge of the structural changes in receptors that lead to G protein coupling. Most GPCR structural analyses have relied on sequence homology alignments [4–6], predictive secondary structural algorithms [7], or molecular engineering approaches [8–11]. Atomic resolution correlates of the pathway of receptor activation are available only for BR and rhodopsin [12,13]. Structural analyses that could reveal ligand binding determinants and confirm the existence of functional GPCR substates have not been possible because protein expression systems do not generate adequate quantities of GPCRs [14–16]. For this reason, this laboratory has endeavored to develop a prokaryotic GPCR expression system that exploits the naturally high levels of expression of the *bacterio-opsin* gene (*bop*).

The *bop* gene is highly expressed in the Archaeon *Halobacterium salinarum*. The bacterio-opsin protein (Bop) couples with the chromophore retinal in a 1:1 stoichiometric ratio [17]. This complex was named bacteriorhodopsin (BR) because, at the time of its discovery, the only other known retinal binding protein was the visual pigment rhodopsin [17]. BR accumulates to levels as high as 15–30 mg/l cell culture and forms a specialized brightly colored membrane (the purple membrane, PM; Ref. [18]). The PM is densely packed, contains 10 lipid molecules per BR monomer, and spontaneously forms two-dimensional crystalline lattices in vivo which facilitate BR purification, functional and structural analyses [18,19].

Some of the most dramatic successes in membrane protein expression have resulted from expression of BR homologues in *H. salinarum*. Under the control of the *bop* gene promoter, numerous BR mutants, halorhodopsin and sensory rhodopsins have been expressed in functional form in yields of 0.5–30 mg protein/l culture [20–23]. Because *H. salinarum* membranes can accommodate very high levels of BR and its homologues, this organism may be suited for expressing non-native seven membrane spanning proteins. Exploiting this expression system is feasible since the *bop* gene has been cloned [24] and some molecular determinants of *bop* gene expression have been characterized. The *bop* gene transcriptional promoter, putative regulatory factor binding sites, and transcriptional terminator have been identified [25–27]. Translational regulation of *bacterio-opsin*, via a signal recognition particle-dependent mechanism, has also been demonstrated [28]. This membrane targeting sequence may be specific to BR and related homologues, because comparison of the pre-sequences of six halo-archaeal integral membrane proteins revealed a unique motif among the retinal binding proteins [28].

The goal of the current work is to understand how the *bop* gene coding region contributes to high-level accumulation of BR and to apply that insight in the expression of the M_1 subtype of the human muscarinic acetylcholine receptor (mAChR) and human α_{2b} adrenergic receptor (a2bAR). mAChRs monitor activity of the neurotransmitter acetylcholine in the central and parasympathetic nervous systems. The muscarinic family of receptors is comprised of five subtypes (M_1–M_5). The odd-numbered subtypes interact with pertussis toxin-insensitive G proteins, stimulate phospholipase C, promote calcium release from cytoplasmic stores, modulate the activity of ion channels, and stimulate mitogenesis [29,30]. The a2bARs also belong to the GPCR superfamily. Three human α_2-AR subtypes are known: α_{2A}, α_{2B} and α_{2C} [31]. All a2bARs couple to inhibition of adenylyl cyclase and ion channel regulation through the pertussis toxin-sensitive G-proteins G_i and G_o. The a2ARs act mainly by inhibiting neuronal firing and release norepinephrine (NE) and other neurotransmitters in the CNS, but they are also involved in a wide range of functions in peripheral tissues, such as modulation of NE release from sympathetic nerves, smooth muscle contraction and metabolic and endocrine regulation [32,33].

Our strategy to direct M_1 and a2bAR expression involved fusing the coding region of the human *m1* and *a2b* gene to nucleotide sequences involved in the regulation of *bop* gene transcription and translation [34–36]. We have engineered 24 combinations of *bop* and *m1-bop* gene fusions, and 30 *a2b-bop* fusions with various carboxyl-terminal tag modifications and characterized their effect on gene expression. Disruption of the *bop* gene carboxyl-terminal coding region, by addition of nucleotide sequences coding for peptide tags, leads to perturbation in the timing and amounts of accumulation of *bop* mRNA and ultimately the levels of BR that accumulate. Similar perturbations are observed when the tag sequences are included into the carboxyl-terminal coding region of *m1-bop* and *a2b-bop* fusion constructs. While transient expression of a2bAR was observed, the fusions that accumulated mRNA or protein did so at much lower levels than that observed for the wild-type *bop* indicating that additional determinants of high-level accumulation remain to be identified.

2. Materials and methods

2.1. Molecular reagents

All chemicals and salts were reagent-grade and obtained from standard biochemical suppliers. T4 DNA ligase and various restriction endonucleases for cloning were purchased from New England Biolabs (Beverly, MA) or from Boehringer Mannheim (Indianapolis, IN). Amplitaq DNA

polymerase was obtained from Perkin-Elmer (Norwalk, CT). Custom oligo-deoxynucleotide primers for mRNA probes and vector constructions were purchased from Gibco (Life Technologies, Gaithersburg, MD).

[*Ethyl*-^{3}H]RS79948-197 (specific activity 81.0 Ci/mmol) and [^{3}H]RX821002 (specific activity 67.0 Ci/mmol) were obtained from Amersham Pharmacia Biotech. [*Methyl*-^{3}H]Rauwolscine (specific activity 77.5 Ci/mmol) was purchased from NEN Life Science Products. Phentolamine was supplied from Sigma Chemicals. Optiphase III liquid scintillation cocktail and glass fiber filtermat were supplied by Perkin-Elmer Life Sciences Wallac Ltd.

Electrophoresis-grade agarose for DNA and RNA gel electrophoresis was from FMC Corporation (Rockland, ME). Nylon Hybond membranes (Amersham, MA) were used for RNA gel blots. TRIzol reagent for RNA extraction was from Life Technologies.

2.2. Carboxyl-terminal-tagged Bop

A 1.2-kilobase-pair DNA fragment containing the wild-type *bop* gene coding region and transcriptional regulatory elements was the basis of our expression strategy (pENDS *bop*I; Ref. [34]). Five additional configurations of the *bop* gene carboxyl-terminal coding region were constructed (Table 1). An endogenous *Not*I DNA restriction site exists within the downstream coding region of the *bop* gene, 73 base pairs (bp) upstream from an engineered *Bam*HI cloning site. The *Not*I–*Bam*HI fragment contains codons for the last five Bop amino acids, the translation stop codon, and 55 bp of noncoding sequence (including the *bop* gene major transcription terminator) [25]. Sequences coding for the carboxyl-terminal HA and 6His tags (*bop:HA* and *bop:6His*, respectively) were inserted immediately upstream of the translation stop codon by polymerase chain reaction (PCR). Oligo-directed mutagenesis (Transformer Site-Directed Mutagenesis kit, Clontech, Palo Alto, CA) was used to introduce a *Cla*I restriction site immediately downstream of the translation stop sequence in pENDS bop I. A positive clone (pENDS *bop:wt-Cla*I) was confirmed by restriction mapping and DNA sequencing. The *Not*I–*Cla*I restriction fragment from pENDS *bop:wt-Cla*I was replaced with pairs of complementary oligos to generate pENDS *bop:6His-Cla*I and pENDS *bop:HA-Cla*I.

2.3. GPCR-Bop fusions

2.3.1. M_1-Bop fusions

Four *m1-bop* fusions (A–D, Fig. 1) were constructed as previously described [34,35]. The "A" fusion included the coding region of the *bop* gene N terminus (including the signal sequence and seven extra-helical amino acid residues) and the last four amino acids of the *bop* gene C terminus. The "B" fusion replaced the entire *m1* extra-helical car-

Table 1
Carboxyl-terminal tag coding regions

Wild Type (WT):

*	A	A	A	T	S	D	*Stop*		
†	GCG	GCC	GCG	ACC	AGC	GAT	*TGA*	TCG	CAC
		Not 1							

Wild Type with *Cla*I (WT-*Cla*I):

A	A	A	T	S	D	*Stop*			
GCG	GCC	GCG	ACC	AGC	GAT	*TGA*	TCG	**AT**C	
	Not 1						*Cla*I		

HA tag (HA):

A	A	A	T	S	**Y**	**P**	**Y**	**D**	**V**	**P**	**D**	**Y**	**A**	*Stop*		
GCG	GCC	GCG	ACC	AGC	TAC	CCA	TAC	GAC	GTC	CCA	GAC	TAC	GCT	*TGA*	TCG	CAC
	Not 1															

HA tag with *Cla*I (HA-*Cla*I):

A	A	A	T	S	**Y**	**P**	**Y**	**D**	**V**	**P**	**D**	**Y**	**A**	*Stop*		
GCG	GCC	GCG	ACC	AGC	TAC	CCA	TAC	GAC	GTC	CCA	GAC	TAC	GCT	*TGA*	TCG	**AT**C
	Not 1														*Cla*I	

6-His tag (6His):

A	A	A	T	S	**H**	**H**	**H**	**H**	**H**	**H**	*Stop*		
GCG	GCC	GCG	ACC	AGC	CAT	CAC	CAT	CAC	CAT	CAC	*TGA*	TCG	CAC
	Not 1												

6-His tag with *Cla*I (6His-*Cla*I):

A	A	A	T	S	**H**	**H**	**H**	**H**	**H**	**H**	*Stop*		
GCG	GCC	GCG	ACC	AGC	CAT	CAC	CAT	CAC	CAT	CAC	*TGA*	TCG	**AT**C
	Not 1											*Cla*I	

* The single letter amino acid code is included above each codon to indicate the C-terminal protein sequence. Bolded amino acids identify engineered tags.
† Nucleotide sequences of downstream coding region. Restriction sites used in the cloning are underlined. The nucleotides shown in boldface were modified to engineer a *Cla*I restriction site.

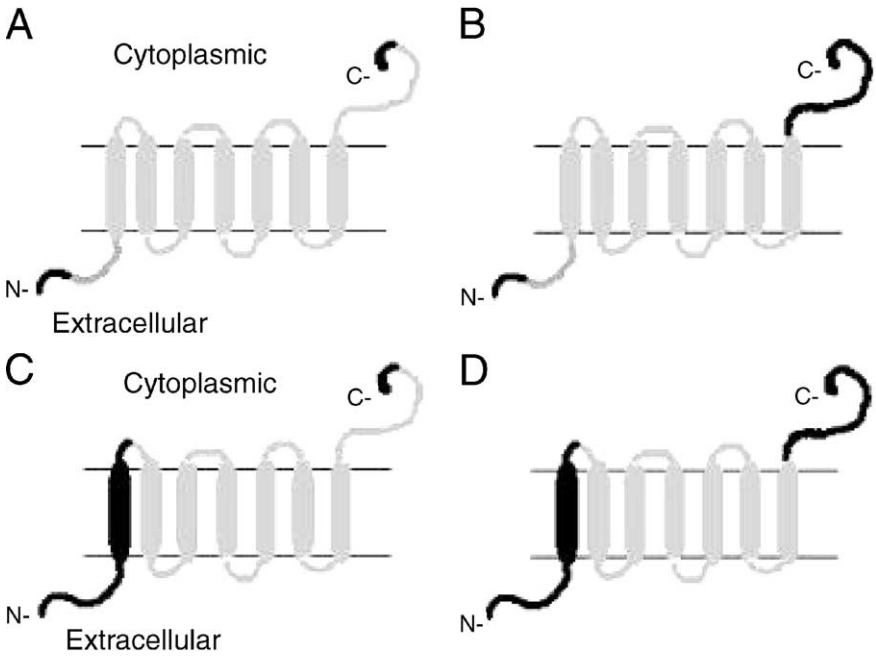

Fig. 1. M_1-Bop fusion proteins. M_1 amino acids are in gray. Bop amino acids are in black. N- and C- refer to the amino and carboxyl termini, respectively. Extracellular and intracellular sides of the membrane are indicated. (A) Minimal fusion. In this configuration, 20 Bop amino acids are fused at the N terminus of M_1. This contains the Bop signal sequence plus seven additional amino acids. Four Bop amino acids remain at the carboxyl-terminal portion of the fusion. (B) C-terminal swap. This fusion adds the 23 C-terminal Bop amino acids after M_1 helix 7. (C) First helix swap. The Bop helix 1 replaces the M_1 helix 1. (D) Combined first helix and C-terminal swap.

boxyl-terminal coding region with the entire extra-helical *bop* gene carboxyl-terminal coding region. The upstream coding region was identical to the "A" fusion. The "C" fusion replaced the entire N-terminal coding region and the first transmembrane helix of the *m1* gene for that of the *bop* gene. The downstream coding region was identical to the "A" fusion. The "D" fusion contained the N terminus using a single unique restriction site within the coding region of the *m1* gene, the first transmembrane helix, and the carboxyl terminal coding regions of the *bop* gene. The *m1-bop* A–D fusions were further modified by subcloning *Not*I–*Bam*HI DNA fragments from the pENDS *bop* constructions containing the six carboxyl-terminal coding regions into each of the four pENDS *m1-bop* cloning vectors.

2.3.2. α_{2B}AR-Bop fusions

Two *a2b-bop* fusions (analogous to B and D, Fig. 1) were constructed. To aid in their construction, unique *Sal*I (introduced immediately downstream of the codon for the initiating methionine), *Hin*dIII (introduced immediately downstream of codon 41 and in-between the coding regions for helices A and B), and *Xho*I (introduced immediately downstream of codon 439) restriction sites were engineered by PCR. The "B" fusion (cloned on a *Sal*I/*Xho*I fragment) contains the coding region of the *bop* gene N terminus (including the signal sequence and extra-helical amino acid residues; 17 residues from *bop* gene). The last 13 residues of the *a2b* C terminus were replaced with the coding region for the 32-residue *bop* gene C terminus. The "D" fusion (cloned on a *Hin*dIII/*Xho*I fragment) replaces the entire N-terminal coding region and first transmembrane helix of the *a2b* gene with codons for the first 47 residues of the *bop* gene. The C-terminal fusion is as in the "B" construct. These two constructs were used as the basis for two deletions in the third intracellular loop (i3) of a2bAR. The first deletion (d1) made use of two fortuitous *Acc*I restriction sites that flanked nearly the entire i3 loop coding region. Digestion with *Acc*I and subsequent religation removed codons 192 through 364. The second deletion (d2) was designed by homology to a functional i3 loop deletion of the human M_1 receptor [37]. The *a2b* contains a unique *Hin*fI site immediately downstream of codon 218. A second *Hin*fI site was engineered after codon 356. Following digestion and religation, codons 218 through 362 were removed. These six *a2b-bop* fusions were further modified by subcloning the *bop:HA*, *bop:6His*, *bop:6His-Cla*I and *bop:HA-Cla*I carboxyl-terminal coding regions into each. All 30 *a2b-bop* constructions were tested for expression in *H. salinarum*.

H. salinarum expression vectors (pHex) were constructed as described [34,35].

2.4. Bacterial strains, media and growth conditions

The *Escherichia coli* and *H. salinarum* strains used and media and culture growth protocols have been described [38]. *H. salinarum* culture media were supplemented with 60

μM scopolamine, an M_1 antagonist, to stabilize expressed M_1 receptors [39], and with 100 μM phentolamine, an a2bAR antagonist, to stabilize expressed a2bARs.

2.5. RNA probes

Digoxygenin-labeled cDNA probes were constructed by PCR (Genius™ system, Boehringer Mannheim). A probe specific for the *H. salinarum* 7S rRNA [40] was included for each blot as an internal control for the total RNA loaded in a gel sample. Densitometric ratios of *bop*, or *m1-bop*, and 7S RNAs (*bop*/7S and *m1*/7S, respectively) were used to compare the levels of mRNA accumulation.

Two *bop* probes were constructed. The first *bop* probe was complementary to the entire *bop* gene coding region (nucleotides 1, the first base of the codon for the initiating methionine, through 825). The second *bop* pre-sequence probe was complementary to the 5′ coding region, nucleotides 1–66. The *m1* probes represent various portions of the *m1* coding region. A 970-bp *m1* probe (referred to as M_1), complementary to the coding region of the *m1* gene from nucleotides 346–1316, was generated by PCR. Three additional *m1* cDNA probes were generated. These included a 184-bp probe complementary to *m1* sequence bases 56–228 (the M_1 first helix), a 121-base probe complementary to bases 233–342 (the M_1 second helix), and a 94-base probe complementary to bases 1255–1338 (the M_1 seventh helix). The *m1* nucleotides were numbered from the first base of the codon for the M_1 amino-terminal methionine.

The *m1B:wt* construction (e.g. *m1-bop* gene "B" fusion with a wild-type *bop* carboxyl-terminal coding region) accumulated significant quantities of *m1-bop* mRNA. Therefore, *m1B:wt* RNA samples were used in gel blot assays to optimize the mixture of M_1 and 7S probes that would allow ratiometric RNA quantification. Once the appropriate concentrations for M_1 and 7S probes were empirically determined, a large pool of combined M1 and 7S probes was generated. All subsequent *m1-bop* mRNA Northern analyses were accomplished using aliquots from this probe pool. The pool of *bop*/7S probes used for all *bop* gene Northern analyses was made in a similar fashion.

The *Sal*I/*Xho*I fragment from the *a2b*B fusion was template for the cDNA probe used in all *a2b-bop* mRNA Northern analyses. The *a2bD:wt* and *a2bD:HA-Cla* constructions (e.g. *a2b-bop* gene "D" fusions with WT and HA-*Cla*I carboxyl-terminal coding regions, respectively) accumulated significant quantities of *a2b-bop* mRNA. Therefore, *a2bD:wt* and *a2bD:HA-Cla* RNA samples were used as controls in the *a2b-bop* gel blot assays to compare the levels of mRNA accumulation.

2.6. RNA isolation and analysis

RNA gel blots were performed to determine mRNA induction time courses and the relative levels of mRNA that accumulated. *H. salinarum* cell samples for RNA analysis were collected from mid-log to late exponential growth stages (A_{660} of 0.8–1.0). Total RNA was isolated as described [38]. Nylon membranes with blotted RNAs were prehybridized for 12 h followed by 12 h of hybridization with a mixture of 7S and *bop*, *m1*, or *a2b* probes in Engler-Blum hybridization solution [0.25 M Na_2HPO_4, 1.0 mM EDTA, 20% sodium dodecyl sulfate (SDS), and 0.5% blocking reagent (pH 7.2, 65 °C)] with gentle rocking. Subsequently, membranes were washed and detected according to a modified Engler-Blum protocol [41]. The modifications included an additional 15-min wash in post-hybridization washing buffer (20 mM Na_2HPO_4, 1.0 mM EDTA, 1.0% SDS) and an additional 15-min wash in washing buffer [0.1 M maleic acid, 3.0 M NaCl, 0.3% Tween (pH 8.0)]. The chemiluminescent substrate CDP-Star™ (NEN, Boston, MA) was used for RNA detection.

Control samples on each *m1-bop* RNA gel blot included *m1B:wt*, *bop:wt* and *L33* (*BR*$^-$). *m1B:wt* mRNA was included on each gel as a control for monitoring the consistency of the probe mixture activity. Because the *bop:wt* mRNA exhibited fortuitous cross-reactivity with all *m1* probes, it was used as an internal control for mRNA size determination. Control samples on each *a2b-bop* RNA gel blot included *a2bB:HA-Cla*I and *a2bB:HA-Cla*I (*d1*).

The bands representing full-length *gpcr-bop* mRNA was determined using known RNA size standards: 23S rRNA (2904 bases), 16S rRNA (1473 bases), 7S rRNA (288 bases) and *bop* mRNA (849 bases). 23S and 16S rRNA sizes were separately visualized by ethidium bromide staining (data not shown). 7S rRNA and *bop* mRNA were visualized by chemiluminescence of the gel blots.

Quantification of mRNA accumulation was accomplished by phosphor imaging (GS 525 Molecular Imager System, Bio-Rad, Hercules, CA) and exposure of the same chemiluminescent gel blots to Kodak X-OMAT AR films (East Rochester, NY). Film images were captured using a computer interfaced CCD camera (AlphaImager IS2000 System). The volumes of the *bop* or *gpcr-bop* and 7S RNA bands were calculated (pixels × area of band) using the "Volume Analysis" function in Multi-Analyst software (Bio-Rad). The pixel volumes were used to determine the *bop*/7S or *m1*/7S ratios. The calculated mRNA/7S ratios, determined by either method, were in close agreement (data not shown) and the average of the obtained mRNA/7S ratios for a specific band was used for subsequent analyses.

2.7. Membrane isolation

Three aliquots of 40–100 ml of cell culture were collected between 24 and 72 h of cell culture growth for protein analysis. Cells were sedimented at 8000 rpm for 20 min. The supernatant was decanted, and cell pellets were resuspended in one-tenth volume basal salts plus scopol-

amine methyl bromide or phentolamine. Cell suspensions were lysed by resuspension in ice-cold incubation buffer [TME: 50 mM Tris–HCl, 10 mM $MgCl_2$, 1 mM EDTA (pH 7.4)] and Complete Proteinase Inhibitor Cocktail (one pellet per 40 ml of cells, Boehringer Mannheim) and either 60 μM scopolamine or 100 μM phentolamine. Cell suspensions were homogenized with an Ultra-Turrax homogenizer (Model T25, Janke and Kunkel, Staufen, Germany; setting 9500 rpm, 3×10 s). Raw membranes were pelleted at $100{,}000 \times g$ for 1 h. Pellets were resuspended in 1 ml of TME buffer. Cell homogenate and membrane were kept at 4 °C and used immediately for protein estimation, ligand binding and Western analysis. Protein concentration was determined using the method of Bradford [42] with bovine serum albumin as the reference standard.

2.8. BR spectroscopy

Membrane fractions containing purified BR (the PM) were isolated by sucrose gradient centrifugation [18]. BR concentration in the PM was quantified using a Perkin-Elmer λ18 spectrophotometer ($\varepsilon_{568}^{BR} = 62{,}700\ M^{-1}\ cm^{-1}$; Ref. [43]) and LabSphere RSA 150 mm light scattering attachment in the diffuse transmittance mode.

2.9. Ligand binding

All incubations were performed in at least duplicate at room temperature. Receptor binding was measured by incubating 25–100 μg of cell homogenate protein or membrane protein with radioligands.

2.9.1. M_1 radioligand binding assays

Membranes were resuspended in 50 mM sodium phosphate buffer containing 1.0 mM EDTA at pH 7.4 and assayed for muscarinic receptors using 1.0 nM [^{3}H]-*N*-methylscopolamine [44].

2.9.2. α_{2B}-AR radioligand binding assays

Homogenates were with [^{3}H]radioligands in a total volume of 100 or 500 μl in TME buffer. After 30 min, the reactions were terminated by dilution in cold buffer and rapid filtration through glass fibre filters using a Tomtec 96 Harvester Mach III (Tomtec, Inc., Hamden, CT) for 100 μl incubations or a Brandel M-48R (Gaithersburg, MD, USA) for 500 μl incubations in a cold room. Filters were washed three times with 5 ml of cold buffer. The bound radioactivity was determined in a MicroBeta liquid scintillation counter (Perkin-Elmer Life Sciences Wallac Ltd.) at 28% efficiency for 100 μl incubations and at 45% efficiency (Model 1410 counter, Perkin-Elmer Life Sciences Wallac Ltd.) for 500 μl incubations. Specific binding was defined as the difference between total and nonspecific binding, determined in a parallel set of reactions but in the presence of an excess of the subtype nonspecific adrenergic receptor antagonist phentolamine (10 μM).

2.10. Bop 5′ polyclonal antibodies and Western analysis

Bop N-terminal amino acids 1–22 comprise the upstream coding region in all pENDS fusion vectors (Fig. 1, Ref. [34]). Therefore, we generated polyclonal antibodies against peptides representative of amino acids 15–22 to assist in the detection of expressed receptors. The peptides (a generous gift from Professor Ed Dratz, Department of Chemistry and Biochemistry, Montana State University) were glutaraldehyde-coupled to keyhole limpet hemocyanin essentially as described [45]. HRP, Inc. (Denver, PA) was contracted to produce polyclonal antisera in New Zealand White female rabbits.

Cell membranes were diluted to an A_{280} of 0.15, solubilized in reducing SDS–polyacrylamide gel electrophoresis (PAGE) gel loading buffer. For solubilization, isolated membrane fractions were solubilized with 1.2% (w/v) *N*-octyl-β-D-glucopyranoside (GERBU, Germany). The samples were incubated overnight at 4 °C on a rotating wheel. The insoluble material was then removed by centrifugation at $200{,}000 \times g$ for 2 h at 4 °C. Cell homogenates, solubilized membrane fractions, or insoluble membrane fraction were separated by 12% SDS-PAGE before being electrotransferred onto polyvinylidene difluoride (PVDF) membrane for immunostaining. For immunostaining, an affinity-purified monoclonal antibody α_{2B}AR-line 7G1 [46], or Bop 5′ polyclonal antibodies were used as a primary antibody (dilution of 1:5000). Immunoreactivity was detected using horseradish peroxidase (HRP)-conjugated anti-mouse antibody (1:20,000) for IgG_1 (Santa Cruz Biotechnology) or HPR-conjugated anti-rabbit (Pierce, Rockford, IL) followed by enhanced chemiluminescence ELC detection kit (Amersham Pharmacia Biotech). Wild-type α_{2B}-AR from *Saccharomyces cerevisiae* [47] and wild-type BR were used as positive and negative controls, respectively. Membranes isolated from L33 were mixed with known quantities of purified PM to calibrate the detection sensitivity of the polyclonal antibodies.

3. Results

3.1. Plasmid stability and culture growth

Southern analysis demonstrated that in all cases, the transformed *H. salinarum* strains maintained the pHex plasmids as autonomously replicating episomes at approximately two to three copies per cell (data not shown). Integration into the *H. salinarum* chromosome was never observed (this study and Ref. [38]). The growth curves for strain L33, L33 expressing the wild-type *bop* gene, the carboxyl-terminally tagged *bop* genes, or the *gpcr-bop* fusions were indistinguishable (data not shown). Therefore, differences in expression levels cannot be ascribed to culture growth or to the instability of the expression constructions, in vivo.

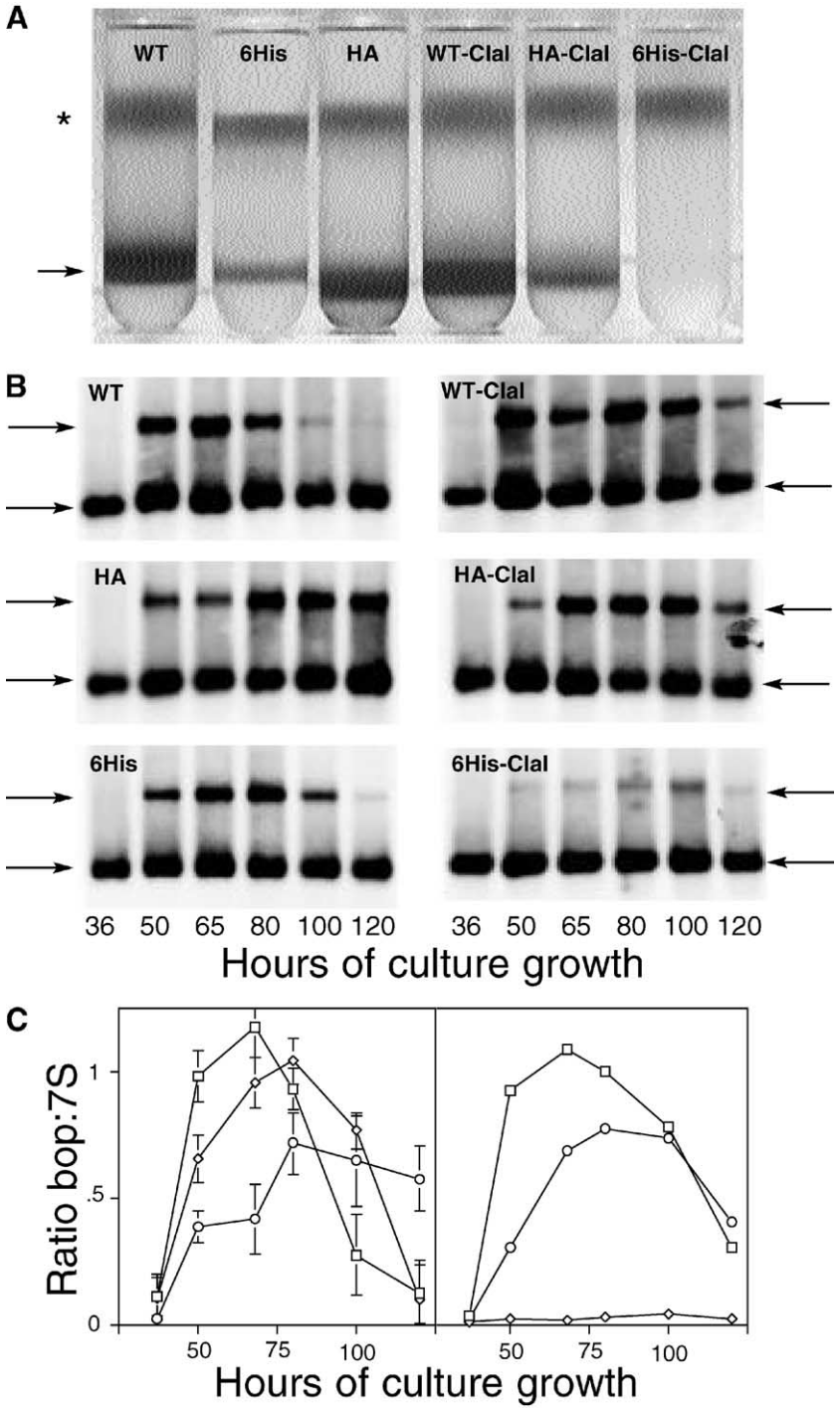

Fig. 2. C-terminal effects on *bop* gene expression. (A) Sucrose gradients used to purify WT, BR:HA, BR:6His, WT-*Cla*I, BR:HA-*Cla*I and BR:6His-*Cla*I. Equivalent OD_{410} nm of whole-membrane preparations were subjected to sucrose density centrifugation. The OD_{410} nm is due to an endogenous membrane-associated cytochrome shown previously to be linearly correlated with cell number [35]. The cytochrome is also used to visually identify the low-density membrane fraction (indicated by *). The high-density band (indicated by arrow) is the PM (purified BR). The intensity at OD_{568} nm was used to determine the quantity of BR that accumulated for each construction, as described in the text. (B) RNA gel blots used to determine *bop* mRNA:7S ratios for *bop:wt*, *bop:HA*, *bop:6His*, *bop:wt-Cla*I, *bop:HA-Cla*I and *bop:6His-Cla*I. Total RNA samples were harvested at the culture growth time point indicated, purified, and blotted onto nylon filters. The cDNA probes used were complementary to the entire *bop* gene coding region (top arrow) and the *H. salinarum* 7S RNA (bottom arrow). The 7S RNA was used as an internal control for gel loading. (C) Ratiometric analysis of *bop*:7S RNAs. The left curves show the means and standard deviations for *bop* mRNA accumulation for three independent cultures expressing *bop* WT (open squares), *bop*:HA (open circles) and *bop*:6His (open diamonds). The right curves show only the means for three independent cultures expressing *bop:wt-Cla*I (open squares), *bop:HA-Cla*I (open circles) and *bop:6His-Cla*I (open diamonds).

Table 2
Effect of downstream coding region variations on BR accumulation

BR construction		BR construction with *Cla*I site
BR:WT[a]	13.4 ± 1.7[b] mg/l[c]	11.8 ± 1.3 mg/l
BR:HA[d]	1.5 ± 1.1 mg/l	2.1 ± 1.4 mg/l
BR:6His[e]	9.9 ± 1.9 mg/l	0

[a] BR:WT, BR with the wild-type carboxyl terminus.
[b] Values are reported as mean and standard deviation from three independent 1.5 l *H. salinarum* cell cultures.
[c] BR concentration (milligrams per liter of cell culture) determined from ε_{568}^{BR} = 62,700 M^{-1} cm^{-1} [43].
[d] BR:HA, BR with carboxyl-terminal HA tag.
[e] BR:6His, BR with carboxyl-terminal HA tag.

3.2. Effect of downstream coding region modifications on bop gene expression

Alterations introduced into the carboxyl-terminal coding region significantly affected *bop* gene expression. Extending the carboxyl-terminal coding region by six consecutive histidines or nine amino acids HA epitope tag reduced BR accumulation to 75% and 11% of wild type, respectively (Fig. 2A, Table 2). Northern analysis demonstrated that the *bop* gene mRNA levels were similarly affected (Fig. 2B,C). The timing of accumulation of the *bop:6His* mRNA was slightly delayed compared to that for the wild type and accumulates to lower maximal levels. The *bop:HA* mRNA accumulated at very reduced mRNA levels and maximal accumulation was delayed by two generation times (>16 h).

The 2-bp change required to generate a *Cla*I DNA restriction site downstream of the *bop* gene translation stop signal had additional effects on expression (Fig. 2, Table 2). In the context of the wild-type coding region, the *Cla*I site modification slightly decreased the maximal levels of

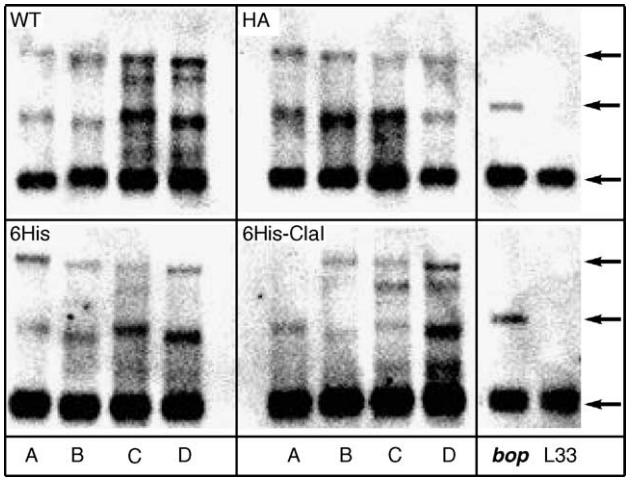

Fig. 3. RNA gel blots used to compare sizes of the *m1-bop* fusion mRNAs. The RNA sample shown for each *m1-bop* fusion was that determined from the time course of induction experiment (Fig. 4) to accumulate maximal full-length mRNA (top arrows). Ten micrograms of total RNA was loaded in each well of the RNA gel blot. The fusions are in the order A, B, C, D, for the carboxyl-terminal coding region fusions WT, HA, 6His and 6His-*Cla*I. *m1-bop* fusion mRNA was identified using a cDNA probe containing the entire *m1* coding region. The *bop* mRNA (middle arrows) for the WT construction showed fortuitous cross-reactivity to this probe. *m1-bop* fusion mRNA (top arrows) was compared with the following RNA size standards, included on the gel: 23S RNA 2904 bases; 16S RNA 1473 bases; *bop wt* 849 bases (middle arrows); 7S RNA 288 bases (lower arrows). The 23S and 16S RNA were visualized by ethidium bromide staining (not shown). The size of the top band corresponds well with the full-length mRNA predicted for each *m1-bop* fusion construction. The molecular origin of the intermediate-sized *m1* specific RNAs was not revealed from our studies. L33 is the *H. salinarum* strain used for all the expression studies and no M_1 probe cross-reactivity is evident.

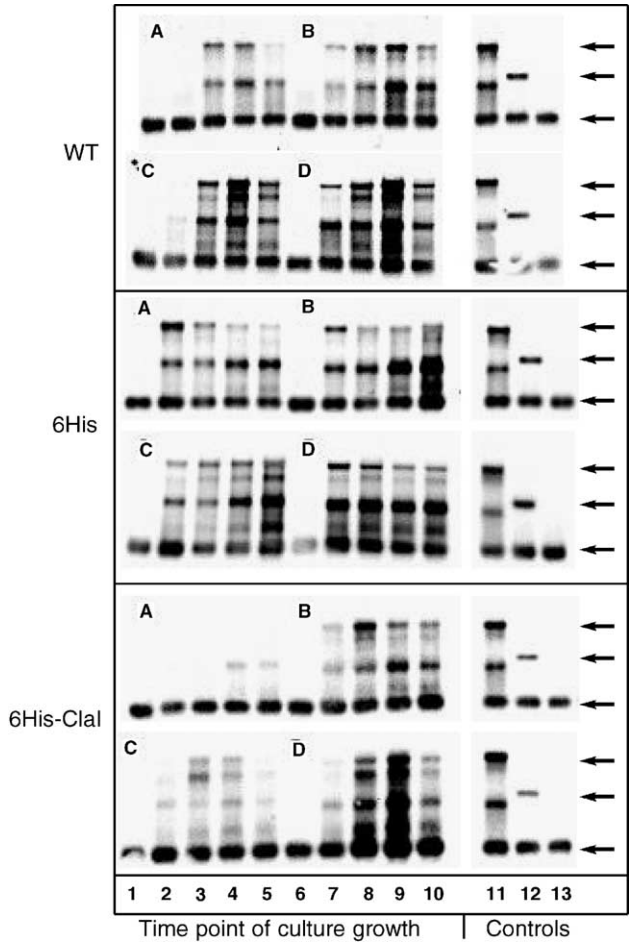

Fig. 4. RNA gel blots of *m1-bop* mRNA for the C-terminal coding region modifications. Only the gel blots for *m1:wt*, *m1:6His* and *m1:6His-Cla*I are shown. Total RNA was isolated from cultures expressing the *m1-bop* gene fusions at the following time points: (1 and 6) 38 h; (2 and 7) 49 h; (3 and 8) 62 h; (4 and 9) 72 h; (5 and 10) 88 h. The cDNA probes used were complementary to the entire *m1* gene coding region (top arrows) and the *H. salinarum* 7S RNA (bottom arrows). The 7S RNA was used as an internal control for gel loading. The *bop* mRNA (middle arrows) for the WT construction showed fortuitous cross-reactivity to the M_1 probe. Each panel shows the effect of carboxyl-terminal coding region modification on all four *m1-bop* gene fusions. Top panel is *m1:wt*; middle panel is *m1:6His*, lower panel is *m1:6His-Cla*I. The symbols A, B, C and D represent the time course of RNA accumulation for the four different *m1-bop* fusions. The three right-most lanes are controls included on each blot: (11) *m1B:wt*, (12) *bop:wt* and (13) L33.

mRNA and protein accumulation. *bop:wt-Cla*I mRNA accumulation remained at maximal levels further into stationary phase. BR:HA-*Cla*I and *bop:HA-Cla*I mRNA accumulated at slightly higher levels than BR:HA and *bop:HA*. In contrast, the *Cla*I site modification in the context of the 6His tag reduced BR and mRNA accumulation to negligible levels. Overall, the order of maximal accumulation of BR and *bop* mRNA was WT ≥ WT-*Cla*I > 6His ≫ HA-*Cla*I ~ ≥ HA ≫ 6His-*Cla*I.

3.3. m1-bop and a2b-bop gene fusions

To determine the contribution of the downstream coding region on heterologous gene expression, we introduced sequences coding for the wild-type Bop carboxyl-terminus (WT), WT-*Cla*I, HA, HA-*Cla*I, 6His and 6His-*Cla*I in the four *m1-bop* gene fusions and the six *a2b-bop* fusions. All 54 constructions were confirmed by restriction mapping and DNA sequencing and expressed in *H. salinarum*.

3.4. gpcr-bop mRNA

RNA gel blots were used to determine the timing and accumulation of the *gpcr-bop* gene mRNAs. Total RNA was isolated from cells during late logarithmic to the early stationary phase of culture growth. The experimentally determined sizes of the full-length *gpcr-bop* fusion mRNAs agreed well with the expected sizes of the full-length mRNAs. We attempted to use the *bop* pre-sequence probe to quantify the relative abundance of the *bop* and *gpcr-bop* mRNAs. The pre-sequence probe detected the *bop:wt* mRNA in 0.05 μg total RNA (data not shown). Using 10 μg total *m1-bopB:wt* RNA or *a2bB:HA-Cla*I RNA, no *gpcr-bop* mRNAs were detected. Therefore, *gpcr-bop* mRNA levels accumulate to significantly lower levels than the wild-type *bop* mRNA.

3.4.1. m1-bop

The M1/7S probe mixture identified only the 7S rRNA in L33 (Figs. 3 and 4). The M_1 probe hybridized with the *bop:wt* mRNA, generating a fortuitous internal size marker useful for identification of full-length *m1-bop* mRNAs. *m1-bop* mRNA accumulated for each of the *m1-bop* fusions. The experimentally determined sizes of the full-length *m1-bop* fusion mRNAs agreed well with the expected sizes of the full-length *m1-bop* mRNAs.

3.4.2. m1-bop RNA conformers

M_1 probe hybridization of total RNA from L33 expressing the *m1-bop* gene fusions revealed the presence of multiple *m1* specific RNA species (Figs. 3 and 4). Some of the smaller *m1-bop* RNA species were abundant. Because we have observed correspondence between BR accumulation and *bop* gene mRNA accumulation, and anticipated a

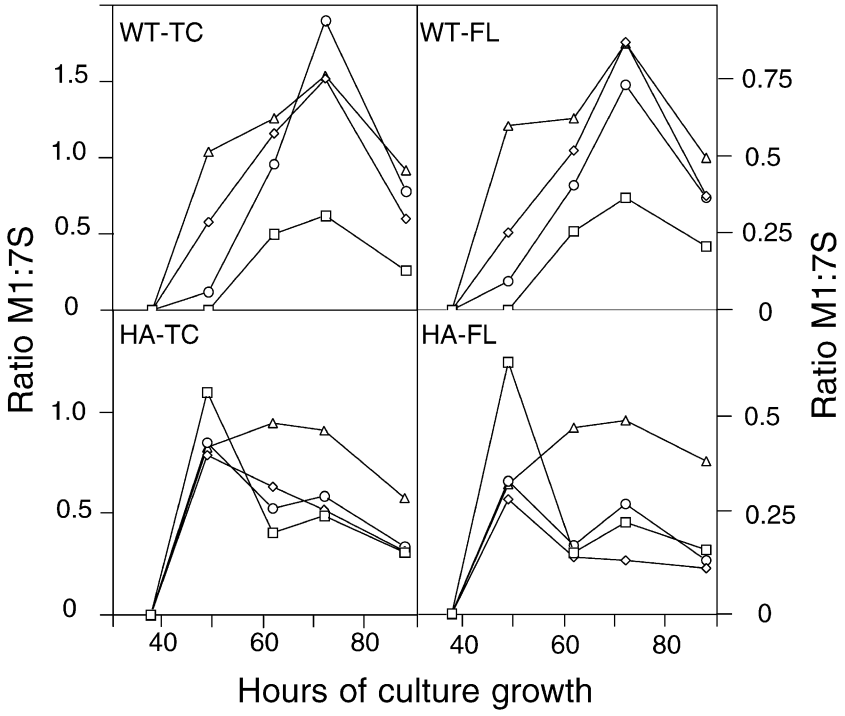

Fig. 5. Time course of accumulation of *m1-bop* mRNA species. The ratios of *m1* mRNA and 7S RNA are plotted versus time of induction. The panels on the left quantify the M1/7S ratios for the total conformer (full-length *m1-bop* mRNA plus the apparent 800-bp *m1-bop* mRNA). The panels on the right quantify the M_1/7S ratios of the full-length *m1-bop* mRNA only. The symbols represent the different *m1-bop* fusions M_1A (open squares), M_1B (open diamonds), M_1C (open circles) and M_1D (open triangles).

similar correspondence for M_1 expression, we attempted to determine the origin of the smaller *m1-bop* RNA species. To determine if the most pronounced band (apparent size ~ 800 bp) was the result of mRNA degradation, a set of *m1* probes was made that were complementary to the coding regions comprising the first, second, and seventh helix of M_1. All probes identified the 800-bp band, suggesting that it is not a degradation product (data not shown). To determine if the 800-bp band was an alternate conformation of full-length *m1* mRNA, a series of RNA denaturation conditions was attempted. None of the denaturation protocols eliminated the 800-bp band (data not shown). The overall trends in *m1-bop* mRNA accumulation were the same whether *m1-bop*/7S ratios for the full-length mRNA or the sum of the 800-bp and full-length *m1-bop*/7S ratios (hereafter termed the total conformer, TC) were quantified (Fig. 5). Until we can rule out that the 800-bp band is not full-length *m1-bop* mRNA, or derived from it, all subsequent quantification of *m1-bop* mRNA refers to the total conformer.

3.4.3. m1-bop mRNA accumulation

The *bop:wt* and *m1B:wt* RNA samples included on each gel blot provided an estimate of the error in mRNA quantification (Figs. 3 and 4). The mean and standard deviation for all *m1B:wt*/7S and *bop:wt*/7S ratios were 1.01 ± 0.07 and 0.58 ± 0.04, respectively ($n = 12$), and demonstrated that the *m1* and 7S probe mixture showed consistent activity.

Table 3
Accumulation of a2:bop fusion mRNA

	a2:bop mRNA	
	B	D
Full-length WT	–	+
HA	–	–
HA-*Cla*I	+	+
6His	–	–
6His-*Cla*I	–	–
d1 WT	+	+
HA	–	–
HA-*Cla*I	+	++
6His	–	+
6His-*Cla*I	–	–
d2 WT	+	+
HA	–	–
HA-*Cla*I	+	+
6His	–	+
6His-*Cla*I	++	–

– mRNA was not observed to accumulate.
+ mRNA was observed to accumulate.
++ mRNA was observed to accumulate at levels higher than other constructions.

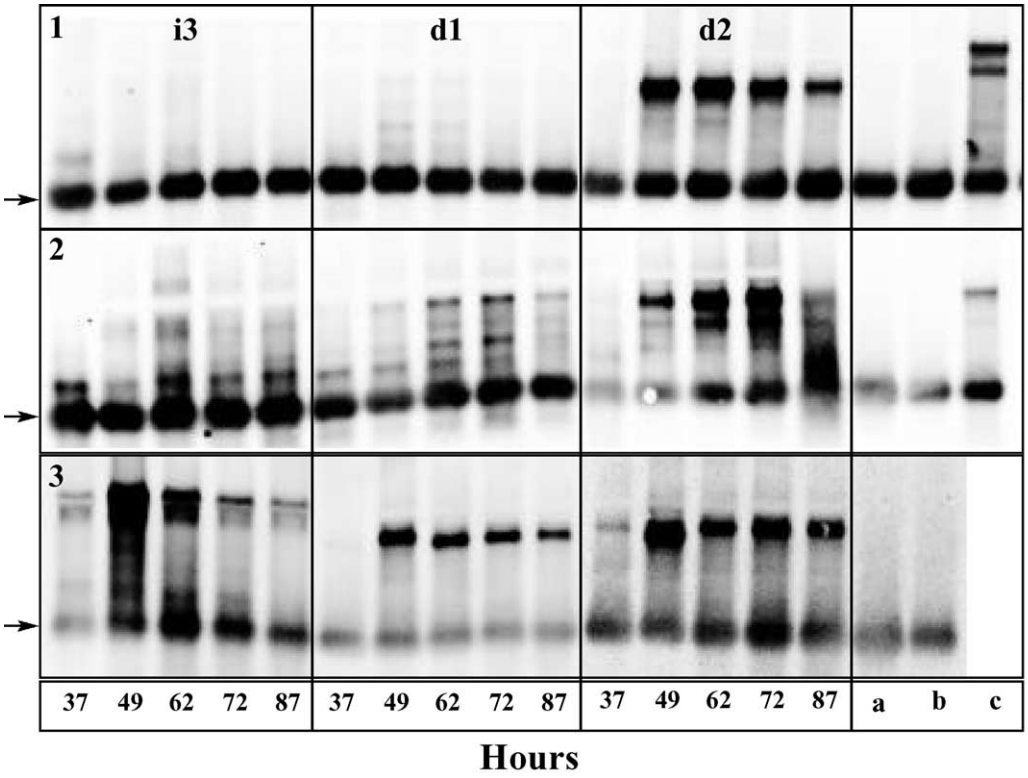

Fig. 6. Time course of accumulation of *a2b-bop* mRNA. Only gel blots for *a2bB:HA* (panel 1), *a2bB:HA-Cla*I (panel 2) and *a2bB:6His-Cla*I (panel 3) are shown. i3 refers to a full-length i3 loop. d1 and d2 refer to the i3 loop deletions as described in the text. Total RNA was isolated at 37, 49, 62, 72 and 87 h of culture growth. Blots were probed with a mixture of the *a2b* and 7S cDNA probes. 7S (indicated by the arrow) was used as a control for gel loading. Additional controls were included on each blot. Panels 1–3 (lanes a and b) are total RNA isolated from *bopI* and L33, respectively. Lanes c include total RNA from cultures expressing *a2bB:HA-Cla*I (panel 1) and *a2bB:HA-Cla*I (d1) (panel 2).

Comparisons of the M1/7S ratios for the different *m1-bop* gene fusions revealed that both the extent of *m1-bop* gene fusions and the carboxyl-terminal modifications affected *m1* mRNA accumulation. mRNA accumulation was inducible for all constructions, detectable quantities of *m1-bop* mRNA did not accumulate until the culture reached mid-log phase of growth (Fig. 4). This induction is similar to that observed for the wild-type *bop* (Fig. 2) [38,48–50].

3.4.4. a2b-bop mRNA

RNA gel blots were also used to determine the timing and accumulation of the *a2b-bop* gene mRNAs. The *a2b* probe identified only *a2b-bop* mRNA in transgenic samples and as observed for *m1-bop* mRNA, accumulation was inducible (Fig. 6). Accumulation of *a2b* mRNA is extremely sensitive to the extent of the *bop* gene fusion and the carboxyl-terminal coding region included (Table 3). A remarkable example is *a2b*B:HA fusion (Fig. 6). Neither is *a2b*B:HA (full-length i3 loop) or is *a2b*B:HA (d1) accumulated detectable mRNA while *a2b*B:HA (d2) accumulated significant quantities. Indeed, at least half of the 30 constructions appeared not to accumulate mRNA. Given the extreme variability and low levels of mRNA that accumulated, the remainder of the *a2b* mRNA analysis was qualitative rather than quantitative. Subsequent analysis of receptor accumulation was performed only for those constructions that accumulated mRNA.

In general, the order of maximal accumulation of *gpcr-bop* mRNA was observed to be WT>WT-*Cla*I ~ 6His>HA>HA-*Cla*I>6His-*Cla*I (Fig. 7, Table 3). These results are similar to those observed for the effects of the same carboxyl-terminal modifications on the levels of accumulation of *bop* mRNA (Fig. 2) and indicate that the downstream coding region contributes to RNA accumulation. The carboxyl-terminal coding regions affording the highest levels of *m1-bop* mRNA accumulation were the WT and 6His (Fig. 7). The carboxyl-

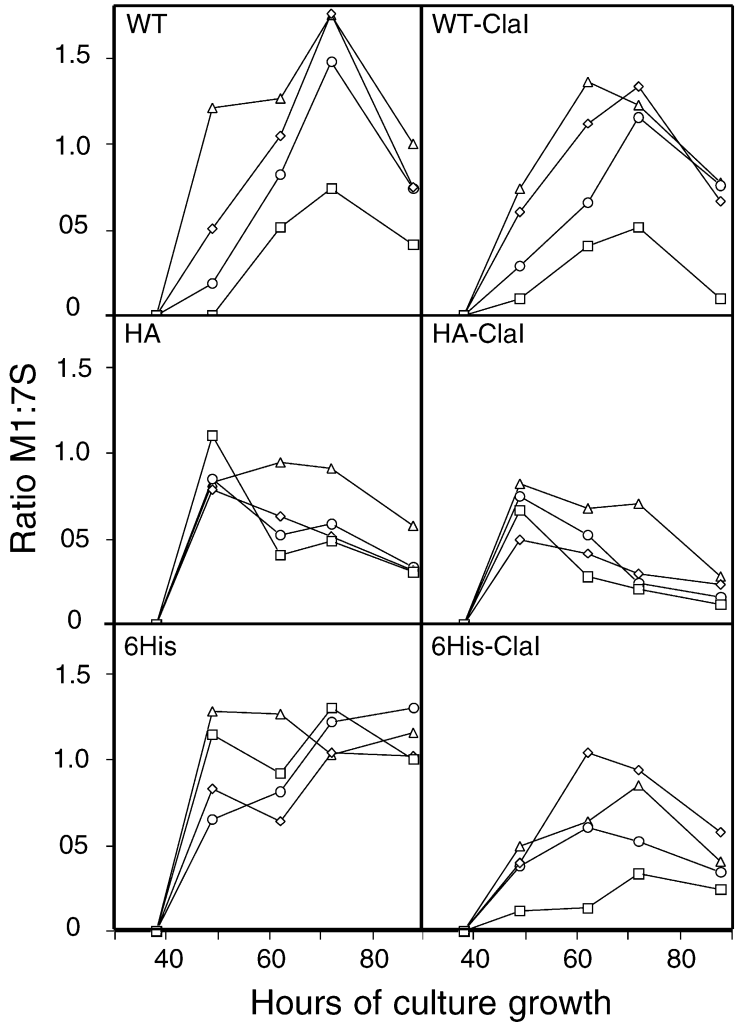

Fig. 7. Time course of accumulation of *m1-bop* mRNA for the C-terminal coding region modifications. The ratios of *m1* mRNA (total conformer) and 7S RNA are plotted versus time of induction. Each panel represents a C-terminal modification for all *m1-bop* gene fusions WT, WT-*Cla*I, HA, HA-*Cla*I, 6His and 6His-*Cla*I. The symbols represent the different *m1-bop* fusions M_1A (open squares), M_1B (open diamonds), M_1C (open circles) and M_1D (open triangles).

terminal coding regions affording the highest levels of *a2b-bop* mRNA accumulation are the WT, HA-*Cla*I and 6His (Table 3).

3.4.5. Effect of bop gene coding region fusions on mRNA accumulation

The patterns of the M1/7S ratios demonstrated that the region of the fused *bop* gene coding region sequences and the carboxyl-terminal region modifications contribute to mRNA accumulation. The effect is not systematic. The M_1A chimeras with WT and 6His-*Cla*I carboxyl-terminal coding regions had the lowest accumulation of mRNA. In contrast, M_1A chimeras with 6His and HA carboxyl-terminal coding regions accumulated the highest levels of mRNA. In the context of the WT and 6His-*Cla*I carboxyl-terminal coding regions, the M_1B, M_1C and M_1D fusions were similar in the timing of induction and levels of mRNA accumulation. The M_1B fusion containing the 6His-*Cla*I carboxyl terminus had the highest mRNA accumulation of all fusions. In the context of the HA and 6His carboxyl terminal coding regions, the M_1B, -C and -D fusions accumulated the least amount of mRNA. In more cases than not, the fusions containing the entire *bop* gene carboxyl-terminal coding region accumulated the most mRNA.

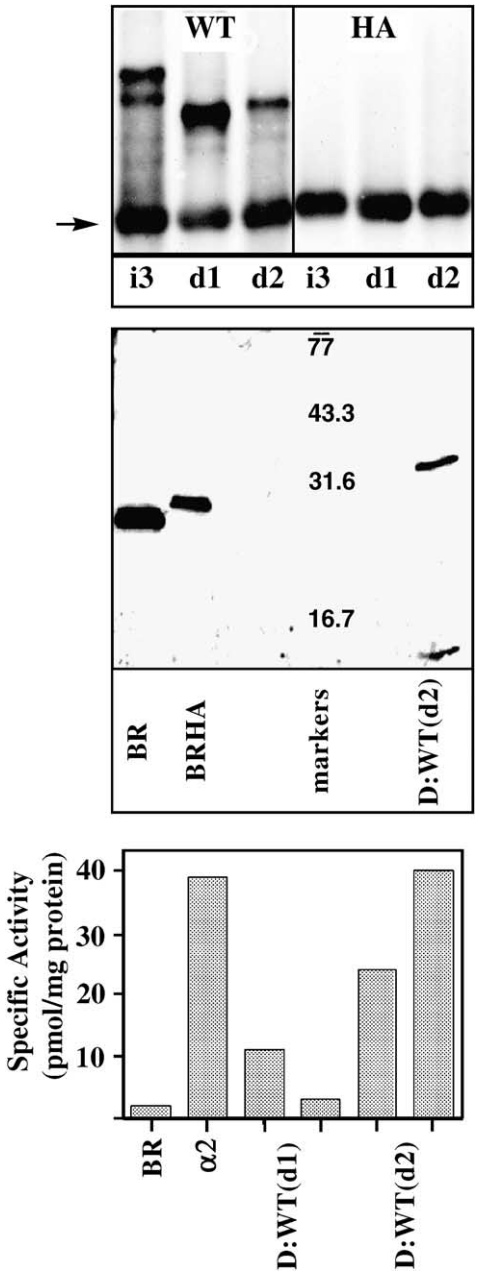

Fig. 8. Functional expression of a2bAR in *H. salinarum* whole membranes. (A) mRNA gel blot of selected *a2b-bop* gene fusions. i3 refers to a full-length i3 loop region. d1 and d2 refer to the i3 loop region deletions as described in the text. Shown in the left panel are three D constructions containing the WT *bop* C-terminal coding region. All have full-length *a2b-bop* mRNA. Shown in the right panel are three constructions containing the HA C-terminal coding region, and none have *a2b-bop* mRNA. (B) Crude membranes were isolated, subjected to SDS gel analysis, and blotted on nylon membranes as described. The bop N-terminal polyclonal antibody was used as the primary antibody. Lanes 1 and 2 are membranes from the positive controls BopI and BopHA, respectively. Lane 3 shows the positions of the molecular weight markers. Lane 4 contains membranes from the a2bD:WT (d2) construction. A positive Western band with a molecular size appropriate for the a2bD:WT (d2) construction is observed near 33 kDa. The smaller band (~ 15 kDa) is likely a proteolytic fragment of the expressed a2bAR. (C) Ligand binding activity of expressed a2bAR in crude *H. salinarum* membranes. Rauwolscine binding was observed for those a2bAR constructions that contained significant quantities of *a2b-bop* mRNA or that were detected in the Western analysis. BR-containing crude membranes were used as negative control. *S. cerevisiae* cell membranes expressing WT a2bAR were used as positive control (α2). Duplicate samples of a2b:WT (d1) and (d2) were observed to bind Rauwolscine with 10-fold lower affinity but at specific activities as high as 40 pmol/mg membrane protein. Membranes from the a2b:HA constructions shown in the right panel of A did not bind Rauwolscine.

3.5. GPCR accumulation

The timing of *bop* gene mRNA and BR accumulation is coupled [38,49] and we anticipate a similar relationship for the *gpcr-bop* fusions. Therefore, we used the results of the *gpcr-bop* mRNA induction analyses to determine the times at which to harvest cell samples for protein analysis. Because maximal *gpcr-bop* mRNA levels are achieved between 40 and 70 h of culture growth, we harvested cells over this time period and prepared membranes for Western analysis and ligand binding.

3.5.1. Westerns

Dilution series of membranes expressing known quantities of BR:WT revealed that the detection limits of the amino-terminal polyclonal antibodies were 20 ng of BR (data not shown). Western analysis of membranes isolated from cultures expressing the M_1-Bop:WT fusion proteins were negative. Membranes isolated from cells expressing a2bD:WT(d2) contained a recombinant protein specifically recognized by the BR polyclonal antibody (Fig. 8). a2b-Bop was not observed for all fusions that accumulated mRNA, suggesting that receptors were expressed at levels below the

antibody detection limits or that receptor accumulation was not stable.

3.5.2. Ligand binding

Ligand binding to membranes prepared from CHO cells expressing M_1 receptors showed normal B_{max} and K_d (data not shown, Ref. [44]). Ligand binding to L33 cell membranes putatively containing the M_1A:Bop and M_1D:Bop (WT and 6His carboxyl-terminal modifications) was negative (data not shown).

[^{3}H]Rauwolscine bound specifically to membranes isolated from some of the a2bAR constructs that accumulate significant quantities of mRNA (Fig. 8). a2bD:WT(d2) bound Rauwolscine at a level of about 40 pmol/mg of membrane protein—a level comparable to that found in *S. cerevisiae* (Fig. 8). As shown by Scatchard plots, this binding affinity is at least 10 times weaker than that of wild-type a2bAR expressed in human or yeast cells (data not shown). The difference cannot be attributed to the i3 loop deletion, as Rauwolscine affinity was unperturbed for a2b-AR (d2) expressed in human cells (data not shown).

4. Discussion

The molecular events that initiate GPCR-mediated signal transduction are not well understood because the structural correlates of receptor activation are largely unknown. The desired structural characterization depends upon obtaining milligram quantities of purified receptors. A logical approach to generate a system for production of GPCRs is to convert a naturally occurring membrane protein expression system to general usage. The Archaeal system under development has many advantages: *H. salinarum* make large quantities of an endogenous membrane protein (BR), this prokaryote is cultured utilizing techniques employed for *E. coli* [26,51], cultures grow under aerophilic conditions that do not require BR for viability, and membranes are quantitatively recovered by centrifugation following hypotonic cell lysis. Work from this laboratory has demonstrated that eubacterial and eukaryotic genes can be expressed at nanogram to milligram levels per liter under the control of the *bop* promoter [22,35]. Using a *bop* gene fusion strategy, functional α_2- and β_2-adrenergic receptors have now been expressed in *H. salinarum* at levels as high as 40 pmol/mg of total membrane protein (Ref. [52]; current study).

While the chromophore retinal provides a useful screen for BR expression, detection of GPCR expression will require tagging strategies. The current work tested the effect of peptide tag modifications on BR expression and revealed that an important determinant of expression is located in the downstream coding region of the *bop* gene. Insertion of DNA coding for a nine-amino-acid HA tag resulted in greater than 90% reduction in *bop:HA* mRNA and BR:HA accumulation. In a separate construction, a 6His coding region resulted in a small reduction in *bop:6His* mRNA and BR:6His accumulation. The resultant perturbations of BR accumulation indicate that expression is sequence dependent. Remarkably, the *bop:6His-Cla*I construction resulted in a near-complete loss of mRNA and protein, indicating an extreme sensitivity to the nucleotide sequence in this region.

The variation observed in tagged *bop* gene expression is not due to codon usage. The *Cla*I site was engineered downstream of the native translation stop sequence and the codons for the 6His tag were not changed in *bop:6His-Cla*I. Therefore, the nucleotide sequence in this coding region contributes to mRNA accumulation and/or protein accumulation by mechanisms that are independent of codon usage preferences. A similar linkage between the carboxyl terminal coding region and angiotensin receptor expression has been observed in mammalian cells [53]. Other observations have shown that carboxyl terminal tag sequences can affect heterologous gene expression in *E. coli*; but in contrast, the effect was attributed to post-translational contributions [54]. Downstream coding region-dependent contributions to expression were also observed during efforts to express the low-abundance BR homologue Sensory Rhodopsin I (SRI) in *H. salinarum*. SRI, under the control of the *bop* gene promoter, engineered essentially as an "A" construction, was expressed at 10% of BR levels. This level of expression was achieved only after truncation of the SRI carboxyl-terminal coding region [21]. SRI shares the same codon usage bias as BR (greater than 65% G/C) so the reduced levels of expression, again, cannot be attributed to codon usage preferences. Krebs et al. [55] added a 6His tag to a similar SRI construction and achieved $\sim$ 20% of BR levels demonstrating, once again, that the context of the tag environment can significantly influence expression levels.

The tag coding regions used do not appear to have perturbed, or introduced, a local nucleotide structure that uniquely contributes to mRNA accumulation. The calculated melting temperature for all six carboxyl-terminal coding regions (from *Not*I site through the major transcription stop site) is 85.4 ± 0.6 °C. Alternatively, the *bop* gene mRNA may form long-range nucleotide interactions (and/or nucleic acid–protein interactions) that contribute to its accumulation.

Inspection of the sequence of the wild-type *bop* mRNA helps to rationalize that the coding region contributes to gene expression. The wild-type *bop* mRNA is $\sim$ 831 nucleotides, 786 ($\sim$ 94%) of which are coding regions [24]. The *bop* mRNA is essentially leaderless; it contains two untranslated bases upstream of the codon for the initiating methionine. There are only $\sim$ 40 noncoding bases between the translation stop and the major transcriptional terminator [25]. If sequences other than the downstream noncoding sequences contribute to mRNA accumulation and translation, they must exist in the coding region. Our expression strategy removes the majority of the *bop* gene coding region. Any *bop* gene coding region determinants that existed will thereby have been perturbed. To date, *gpcr-*

bop gene fusion expression levels are at least an order of magnitude less than that for BR [34–36], supporting our hypothesis that the *bop* gene coding sequences contains critical determinants of expression.

Because the modifications made to the downstream coding region of the *bop* gene resulted in dramatic differences in expression, we anticipated that these same modifications would influence expression of the *gpcr-bop* gene fusions. We found that the levels of *m1-bop* mRNA accumulation depended on both the *gpcr-bop* gene fusion used and on the carboxyl-terminal modification included. Similar to that observed for *bop* gene expression, a range of *gpcr-bop* mRNA accumulation was observed with the carboxyl terminal preference of WT>6His>HA. The total amount of *gpcr-bop* mRNA that accumulated does not systematically correlate with the extent of the *bop* gene coding region contained in each chimera. For example, the *m1-bop:D* fusions, containing the most extensive *bop* gene coding region fusion, did not accumulate the highest levels of mRNA. However, in general, the D fusions consistently accumulated significant levels of mRNA.

While we have been able to manipulate the *gpcr* mRNA levels by addition of *bop* gene and carboxyl-terminal coding sequences, the engineering strategy used was not adequate to achieve wild-type *bop* levels of mRNA accumulation. The absence of detectable M_1 receptors is presumably related to the low levels of mRNA. The levels of the wild-type *bop* mRNA that normally accumulate may result from noncontiguous coding region sequence determinants remote from the transcriptional promoter. It may be necessary to engineer more extensive *m1-bop* coding region chimeras or to pursue molecular evolution strategies to generate coding sequences capable of mimicking *bop* gene determinants of mRNA accumulation. Implementation of the latter strategy is currently in progress.

The timing and the amounts of *bop* and *m1-bop* mRNA that accumulated were observed to vary for the different carboxyl-terminal coding regions. The wild-type *bop* mRNA declined rapidly in the late stationary phase of culture growth, suggesting that *bop* mRNA synthesis is decreased or an increase in *bop* mRNA degradation. It is interesting to note that even though BR:HA and BR:HA-*Cla*I accumulated significant quantities of mRNA in the late stationary phase of cell growth, neither construction accumulated significant protein. This suggests that timing of mRNA accumulation and translation are coupled for *bop* gene expression. The low levels of *m1-bop* mRNA that accumulated are likely a combination of the timing of induction of transcription, transcription termination and mRNA stability. The steady-state accumulation observed for *m1-bop* containing the 6His coding region indicates a role for the carboxyl-terminal coding region in the termination of *bop* mRNA transcription, in the stability of mRNA stability, or both. The differences between the timing of mRNA accumulation for the *bop* and *m1-bop* fusions illustrate a methodological lesson from this work; analysis of heterologous gene mRNA accumulation should be performed to design protein harvesting strategies.

It is evident from immunoblots and ligand binding data that there is unstable a2bAR:BR expression and that [^{3}H]Rauwolscine binds to the fusion proteins with low affinity. The lower binding affinity of the fusion proteins in *H. salinarum* might have numerous origins: (1) absence of G proteins in *H. salinarum*, (2) different lipid composition of *H. salinarum* membranes, or (3) modifications at the N and/or C termini of the receptor fusions influence the gene expression or folding of α_{2B}-AR. Indeed, studies to be reported elsewhere demonstrated that the N-terminal modifications introduced here, but not the C-terminal modifications, perturb α_{2B}-AR accumulation in CHO cells. Further optimization of the N/C-terminal coding region of a2b-bop WT constructs and expression studies are thus necessary for high protein level production of functional intact receptor in the *H. salinarum* system.

In conclusion, this work provides further insight into the expression of non-native genes in a novel prokaryotic expression system. We have demonstrated that *H. salinarum* can express functional eukaryotic GPCRs and that specific coding regions contribute to their potential for expression. The coding region influence appears to be at the nucleotide level and is not due to codon usage preferences. The combinations of *bop* gene fusions and C-terminal coding region modifications attempted did not result in systematic improvements in receptor expression, indicating that nucleotide sequence-dependent determinants of expression are not local in nature. We have observed that for wild-type BR, and thus likely for GPCR, mRNA and receptor accumulation are tightly coupled and this coupling can be perturbed by small changes in coding sequences. The available BR N-terminal polyclonal antibodies will direct our future studies on constructions containing poly-His coding regions. Successful optimization of this strategy will result in production of the amounts of receptor proteins required to achieve a structure-based understanding of GPCR function. In the process, principles of high-level expression in the third domain of life, the Archaea, will be revealed.

Acknowledgements

The authors acknowledge Ann Winter-Vann and Mika Rantanen for help in making the muscarinic and adrenergic constructs, respectively.

References

[1] A. Wise, K. Gearing, S. Rees, Drug Discov. Today 7 (2002) 235–246.
[2] A.G. Gilman, Annu. Rev. Biochem. 56 (1987) 615–649.

[3] P.A. Hargrave, Curr. Opin. Struct. Biol. 1 (1991) 575–581.
[4] J.M. Baldwin, G.F. Schertler, V.M. Unger, J. Mol. Biol. 272 (1997) 144–164.
[5] R. Link, D. Daunt, G. Barsh, A. Chruscinski, B. Kobilka, Mol. Pharmacol. 42 (1992) 16–27.
[6] Y.H. Feng, K. Noda, Y. Saad, X.P. Liu, A. Husain, S.S. Karnik, J. Biol. Chem. 270 (1995) 12846–12850.
[7] J. Kyte, R.F. Doolittle, J. Mol. Biol. 157 (1982) 105–132.
[8] S.A. Hjorth, H.T. Schambye, W.J. Greenlee, T.W. Schwartz, J. Biol. Chem. 269 (1994) 30953–30959.
[9] E. Burstein, T. Spalding, D. Hill-Eubanks, M.R. Brann, Biol. Chem. 270 (7) (1995) 3141–3146.
[10] Y. Yamano, K. Ohyama, M. Kikyo, T. Sano, Y. Nakagomi, Y. Inoue, N. Nakamura, I. Morishima, D.F. Guo, T. Hamakubo, T. Inagami, J. Biol. Chem. 270 (1995) 14024–14030.
[11] C. Wang, S. Jayadev, J.A. Escobedo, J. Biol. Chem. 270 (1995) 16677–16682.
[12] J.K. Lanyi, Biochemistry (Mosc.) 66 (2001) 1192–1196.
[13] K. Palczewski, T. Kumasaka, T. Hori, C.A. Behnke, H. Motoshima, B.A. Fox, I. Le Trong, D.C. Teller, T. Okada, R.E. Stenkamp, M. Yamamoto, M. Miyano, Science 289 (2000) 739–745.
[14] R. Grisshammer, C.G. Tate, Q. Rev. Biophys. 28 (1995) 315–422.
[15] G.F.X. Schertler, Curr. Opin. Struct. Biol. 2 (1992) 534–544.
[16] R. Laage, D. Langosch, Traffic 2 (2001) 99–104.
[17] D. Oesterhelt, W. Stoeckenius, Nature 233 (1971) 149–154.
[18] D. Oesterhelt, W. Stoeckenius, Methods Enzymol. 31 (1974) 667–678.
[19] N. Grigorieff, T.A. Ceska, K.H. Downing, J.M. Baldwin, R. Henderson, J. Mol. Biol. 259 (1996) 393–421.
[20] J.A. Heymann, W.A. Havelka, D. Oesterhelt, Mol. Microbiol. 7 (1993) 623–630.
[21] E. Ferrando-May, B. Brustmann, D. Oesterhelt, Mol. Microbiol. 9 (1993) 943–953.
[22] G.J. Turner, L.J. Miercke, A.K. Mitra, R.M. Stroud, M.C. Betlach, A. Winter-Vann, Protein Expr. Purif. 17 (1999) 324–338.
[23] L.C. Martinez, R.L. Thurmond, P.G. Jones, G.J. Turner, Proteins 48 (2002) 269–282.
[24] R. Dunn, J. McCoy, M. Simsek, A.S.C. Majumdar, U. RajBhandary, H.G. Khorana, Proc. Natl. Acad. Sci. U. S. A. 78 (1981) 6744–6748.
[25] S. DasSarma, U.L. RajBhandary, H.G. Khorana, Proc. Natl. Acad. Sci. U. S. A. 81 (1984) 125–129.
[26] M.C. Betlach, R.F. Shand, in: F. Rodriguez-Valera (Ed.), General and Applied Aspects of Halophilic Microorganisms, Plenum, New York, 1991, pp. 259–264.
[27] N.S. Baliga, S. DasSarma, J. Bacteriol. 181 (1999) 2513–2518.
[28] R. Gropp, F. Gropp, M. Betlach, PNAS 89 (1992) 1204–1208.
[29] E.M. Ross, G. Berstein, Life Sci. 52 (1993) 413–419.
[30] E.V. Stephens, G. Kalinec, M.R. Brann, J.S. Gutkind, Oncogene 8 (1993) 19–26.
[31] D.B. Bylund, H.S. Blaxall, L.J. Iversen, M.G. Caron, R.J. Lefkowitz, J.W. Lomasney, Mol. Pharmacol. 42 (1992) 1–5.
[32] H. Kurose, J.W. Regan, M.G. Caron, R.J. Lefkowitz, Biochemistry 30 (1991) 3335–3341.
[33] L.E. Limbird, FASEB J. 2 (1988) 2686–2695.
[34] G.J. Turner, R. Reusch, A.M. Winter-Vann, L. Martinez, M.C. Betlach, Protein Expr. Purif. 17 (1999) 312–323.
[35] A.M. Winter-Vann, L. Martinez, C. Bartus, A. Levay, G.J. Turner, in: S. Kiihne, H.J.M. de Groot (Eds.), Perspectives on Solid State NMR in Biology, Kluwer, Dordrecht, The Netherlands, 2001, pp. 141–160.
[36] C.L. Bartus, Biology, University of Miami, Miami, 2000, p. 63.
[37] J.R. Arden, O. Nagata, M.S. Shockley, M. Philip, J. Lameh, W. Sadee, Biochem. Biophys. Res. Commun. 188 (1992) 1111–1115.
[38] A.M. Winter-Vann, L. Martinez, L. Parker, J. Talbot, G.J. Turner, Cancer Res. Ther. Control 8 (1999) 275–289.
[39] U. Gether, J.A. Ballesteros, R. Seifert, E. Sanders-Bush, H. Weinstein, B.K. Kobilka, J. Biol. Chem. 272 (1997) 2587–2590.
[40] A. Moritz, B. Lankat-Buttgereit, H. Gross, W. Goebel, Nucleic Acids Res. 13 (1985) 31–43.
[41] G. Engler-Blum, M. Meier, J. Frank, G.A. Muller, Anal. Biochem. 210 (1993) 235–244.
[42] M.M. Bradford, Anal. Biochem. 72 (1976) 248–254.
[43] M. Rehorek, M.P. Heyn, Biochemistry 18 (1979) 4977–4983.
[44] L. Potter, D. Flynn, H. Hanchett, D. Kalinoski, J. Luber-Narod, D. Mash, Trends Pharmacol. Sci. Suppl. (1984) 22–31.
[45] E. Harlow, D. Lane, Using Antibodies: A Laboratory Manual, Cold Spring Harbor Laboratory Press, Cold Spring Harbor, NY, 1999.
[46] S. Liitti, H. Narva, A. Marjamaki, J. Hellman, J. Kallio, M. Jalkanen, M.T. Matikainen, Biochem. Biophys. Res. Commun. 233 (1997) 166–172.
[47] A. Kapat, V.P. Jaakola, H. Heimo, S. Liitti, P. Heikinheimo, T. Glumoff, A. Goldman, Bioseparation 9 (2000) 167–172.
[48] C.-F. Yang, S. DasSarma, J. Bacteriol. 172 (1990) 4118–4121.
[49] R.F. Shand, M.C. Betlach, J. Bacteriol. 173 (1991) 4692–4699.
[50] R.F. Shand, M.C. Betlach, J. Bacteriol. 176 (1994) 1655–1660.
[51] S. DasSarma, E.M. Fleischmann, in: F.T. Robb (Ed.), Archaea, A Laboratory Manual, vol. 3, Cold Spring Harbor Laboratory Press, Cold Spring Harbor, 1995, pp. 1–280.
[52] P. Sohlemann, J. Soppa, D. Oesterhelt, M.J. Lohse, Naunyn-Schmiedeberg's Arch. Pharmacol. 355 (1997) 150–160.
[53] Z. Gaborik, B. Mihalik, S. Jayadev, G. Jagadeesh, K.J. Catt, L. Hunyady, FEBS Lett. 428 (1998) 147–151.
[54] J. Tucker, R. Grisshammer, Biochem. J. 317 (1996) 891–899.
[55] M.P. Krebs, E.N. Spudich, J.L. Spudich, Protein Expr. Purif. 6 (1995) 780–788.